

## *N,N-Dimethyl chitosan/heparin polyelectrolyte complex vehicle for efficient heparin delivery*



Pedro V.A. Bueno<sup>a</sup>, Paulo R. Souza<sup>a</sup>, Heveline D.M. Follmann<sup>a</sup>, Antonio G.B. Pereira<sup>a,b</sup>, Alessandro F. Martins<sup>a,b,\*</sup>, Adley F. Rubira<sup>a</sup>, Edvani C. Muniz<sup>a</sup>

<sup>a</sup> Grupo de Materiais Poliméricos e Compósitos, GMPC, Departamento de Química, Universidade Estadual de Maringá UEM, Av. Colombo 5790, CEP 87020-900 Maringá, Paraná, Brazil

<sup>b</sup> Universidade Tecnológica Federal do Paraná (UTFPR), Estrada para Boa Esperança, CEP 85660-000 Dois Vizinhos, Paraná, Brazil

### ARTICLE INFO

#### Article history:

Received 22 December 2014

Received in revised form 16 January 2015

Accepted 19 January 2015

Available online 24 January 2015

#### Keywords:

*N,N*-Dimethyl chitosan

Heparin

Polyelectrolyte complex

### ABSTRACT

Polysaccharide-based device for oral delivery of heparin (HP) was successfully prepared. Previously synthesized *N,N*-dimethyl chitosan (DMC) (86% dimethylated by <sup>1</sup>H NMR spectroscopy) was complexed with HP by mixing HP and DMC aqueous solutions (both at pH 3.0). The polyelectrolyte complex (PEC) obtention was confirmed by infrared spectroscopy (FTIR), thermogravimetric analysis (TGA/DTG) and wide-angle X-ray scattering (WAXS). In vitro controlled release assays of HP from PEC were investigated in the simulated intestinal fluid (SIF) and simulated gastric fluid (SGF). The PEC efficiently protected the HP in SGF condition in which HP is degraded. On the other hand, in SIF PEC promoted the releasing of 80 ± 1.5% of loaded HP. The promissory results indicated that the PEC based on DMC/HP presented potential as drug-carrier matrix, since biological activity of HP was improved at pH close to physiological condition.

© 2015 Elsevier B.V. All rights reserved.

### 1. Introduction

Heparin (HP) is a linear biopolymer that consists of sulfated D-glucosamine units, joined in alternating sequence by  $\alpha$ (1,4)-glycosidic linkages, to either D-glucuronic or L-iduronic acid [1,2]. HP is an anionic polysaccharide that, at specific conditions of pH, could be used to form polyelectrolyte complexes (PECs) with cationic polymers [3–5]. HP presents many applications in medical and pharmaceutical areas. It acts indirectly in the blood coagulation mechanism, stimulates cellular growth and has antibacterial effects [3–5]. However, low molecular weight heparin (LMWHP) does not present effective anticoagulant activity [6]. The administration of HP is performed by intravenous or subcutaneous routes for it does not exist an efficient oral method, since HP degradation occurs in the gastrointestinal tract (GIT) [7]. In addition, high molecular mass and low lipophilicity of HP, reduces its absorption on GIT epithelial membrane cells [7]. GIT epithelium acts as a physical and chemical barrier toward the absorption of proteins and peptides, restricting the entry of macromolecules into systemic circulation [7].

On the other hand, conventional methods of administration (intravenous or subcutaneous routes) lead to side effects [2]. Heparin-induced thrombocytopenia (HIT), hemorrhage and osteoporosis are the adverse effects most commonly observed after HP administration [8,9]. The HIT is defined when the platelet count decreases 50% in relation to the platelet count prior of HP treatment [9]. Patients that receive high amounts of HP (15,000 to 30,000 IU kg<sup>-1</sup> daily) in periods over six months can develop osteoporosis [10]. However, the mechanism by which the HP produces the osteoporosis is uncertain. Studies have suggested that HP binds to the calcium ions and prevents calcification [11]. Therefore, to transpose these problems is essential developing an efficient HP delivery device by the oral route. Compared to the conventional methods of administration, delivery of drugs via the oral route is relatively simple and non-invasive [7]. In this case, medication can be easily administered and also avoid the risk of blood infections or injury associated to the conventional methods of administration. In addition, oral administration occurs with absence of needle and consequently this administration method is preferred due to its improved convenience and patient compliance [7,12].

Chitosan (CHT) is a polysaccharide obtained from partial deacetylation of chitin. CHT appears as a promising biopolymer having unmatched features, including biocompatibility, biodegradability and antimicrobial properties with potential application in advanced materials varying from tumor cells recognition and

\* Corresponding author at: Universidade Tecnológica Federal do Paraná (UTFPR), Estrada para Boa Esperança, CEP 85660-000 Dois Vizinhos, Paraná, Brazil.  
Tel.: +55 46 3536 8413; fax: +55 46 3536 8900.

E-mail address: [afmartins50@yahoo.com.br](mailto:afmartins50@yahoo.com.br) (A.F. Martins).

sustained release of drugs [1,13,14]. CHT/polyanionic polymer PECs are widely used as implant devices and as drugs release vehicles [15,16]. CHT uses are limited, although there are many studies on the use of CHT as drug carriers. This fact occurs due to its low solubility at pH 7.4 [14], reduced mucoadhesion and a poor membrane cell permeation above pH 6.5 [1,17,18]. Combining or preparing CHT-derivatives is a rational pathway to overcome CHT solubility restrictions generating new materials with wider applications than those presented by conventional CHT-based materials [19,20].

*N,N,N*-Trimethyl chitosan (TMC), the simplest form of quaternized CHT, has greater antimicrobial action, mucoadhesivity and permeability in relation to CHT and it is water soluble even at pH > 7 [1,17]. Follmann et al. [21] developed antimicrobial and anti-adhesive TMC/HP films by LbL on chemically modified polystyrene substrates. According to reports, one can verify a diversity of studies and applications using CHT and/or CHT-derivatives, specially on controlled drug release fields [22–25]. TMC has better mucoadhesion property regarding CHT due to *N*-trimethylation of amino groups that provides permanent positively charged sites [18,26]. Besides, the free rotation of the C-H bonds as well as the hydrophobic nature of methyl groups increase the permeability and mucoadhesivity of TMC-based materials on epithelial cells [18,26]. HP degradation can be inhibited in GIT and permeation enhancer in the intestinal epithelium can be achieved by new polymeric systems (hydrogels) with stimuli-responsive and mucoadhesive properties [7].

On the other hand, TMC/heparin (TMC/HP) PECs are not suitable HP carrier at physiological pH. In vitro release studies showed the TMC/HP complex only protects HP on gastric condition and represses drug release on physiological conditions [1,2]. TMC has *N*-quaternized  $[-^4\text{N}(\text{CH}_3)_3]$  groups that display permanent charges at any pH. Therefore, the electrostatic interactions among such sites with  $-\text{COO}^-$  and with  $-\text{OSO}_3^-$  groups of HP are permanent at pH 7.4. So, the release of HP from TMC/HP complex is suppressed in this condition due to the *N*-quaternization of the amino groups [1,2].

*N,N*-Dimethyl chitosan (DMC) does not have *N*-trimethylated groups in its backbone. In this case, controlled release systems based on DMC can be advantageous over TMC, considering the electrostatic interactions on DMC/HP PEC could be undone at physiological pH, improving HP releasing. So, DMC/HP PEC can maintain the HP structure when subjected to gastric condition and at the same time act as an efficient vehicle for HP at pH close to physiological condition. This paper describes, for the first time, the association of DMC with a system formed by a polyelectrolyte complex of DMC/HP at pH 3.0. The release studies of heparin (HP) from DMC/HP complex matrix was evaluated in simulated gastric fluid (SGF) and simulated intestinal fluid (SIF).

## 2. Materials and methods

### 2.1. Materials

Chitosan (85% deacetylated;  $\bar{M}_w$  of  $8.7 \times 10^4 \text{ g mol}^{-1}$ ) was purchased from Golden-Shell Biochemical (China). Heparin sodium ( $\bar{M}_w$ , of  $14 \times 10^3 \text{ g mol}^{-1}$ ) was kindly supplied by Kin Master (Brazil). Cellulose membrane (molecular weight cut off: 12 kDa) used for dialysis, was purchased from Sigma-Aldrich (Brazil). Other reagents, such as sodium hydroxide, formaldehyde and formic acid were used as purchased without further purification.

### 2.2. Synthesis of *N,N*-dimethyl chitosan (DMC)

*N,N*-Dimethyl chitosan was synthesized based on method reported by Matins et al. [27], with some adaptations. Initially, 10 g of CHT, 30 mL of formic acid, 40 mL of formaldehyde and 180 mL

of distilled water were added to a 500 mL one neck round flask. The system was kept under reflux at 70 °C for 120 h under magnetic stirring, and a yellow viscous solution was obtained. The yielded material was precipitated in NaOH solution (1.0 mol L<sup>-1</sup>), and the formation of a gel was observed. The gel was washed with deionized water to remove the impurities and then dissolved in dilute aqueous HCl solution (pH ≈ 4.0). This solution was dialyzed against deionized water for five days and the DMC was frozen and lyophilized.

### 2.3. Preparation of polyelectrolyte complex of DMC/HP

PEC was obtained at pH 3.0 and the volume ratio of DMC-solution to HP-solution was kept constant. The following procedure was adopted: stock aqueous solutions of DMC (2.0 g in 200 mL of acetic acid/sodium acetate buffer solution) and HP (4.0 g in 200 mL of acetic acid/sodium acetate buffer solution) were prepared. Afterward, 20 mL of the previously DMC-solution (1.0% w/v) was slowly dropped into HP-solution (20 mL, 2.0% w/v) at room temperature and under magnetic stirring, keeping the volume ratio at 1/1 (DMC-solution/HP-solution). The formed material was washed with deionized water and separated by centrifugation (30 min, 9500 rpm at 2.0 °C). Then, the precipitate was washed with distilled water, frozen and lyophilized at –55 °C for 48 h.

## 2.4. Characterization

### 2.4.1. <sup>1</sup>H nuclear magnetic resonance spectroscopy

<sup>1</sup>H NMR spectra were performed on a Varian, Mercury Plus 300 BB NMR spectrometer (USA), operating at 300 MHz for <sup>1</sup>H frequency. For the acquisition of <sup>1</sup>H NMR spectra, 10 mg of CHT or DMC were dissolved in 1.0 mL of D<sub>2</sub>O/CD<sub>3</sub>COOD (100/1 v/v). Spectra were acquired at room temperature, and the main acquisition parameters were as follows: a pulse of 45°; a recycle delay of 10 s and acquisition of 128 transients. Time-domain data were apodized with a 0.2 Hz exponential function (lb) to improve the signal-to-noise ratio before Fourier transformation. The dimethylation degree (DD) of DMC was determinate through <sup>1</sup>H NMR spectrum. The result was obtained using the equation below [28].

$$\text{DD\%} = \frac{[(\text{CH}_3)_2]}{6[\text{H}2]} \times 100 \quad (1)$$

where  $[(\text{CH}_3)_2]$  is the integral of *N*-dimethylated amine groups at 3.10 ppm;  $[\text{H}2]$  is the integral of the H2 at 3.43 ppm, signal related to the hydrogen atoms bound to the C2 of the DMC molecule (see DMC <sup>1</sup>H NMR spectrum in Fig. 1b).

### 2.4.2. FTIR spectroscopy

FTIR was used to characterize the chemical structure of materials (DMC, HP and PEC). In each case, KBr disk with 1.0 wt% of the sample was prepared. The equipment from Shimadzu Scientific Instruments (Model 8300, Japan) was used at the following conditions: range of 4000–500 cm<sup>-1</sup>, resolution of 4 cm<sup>-1</sup> obtained after cumulating 64 scans.

### 2.4.3. Wide angle X-ray scattering (WAXS)

WAXS profiles were recorded on a Shimadzu diffractometer model XRD-600 equipped with a Ni-filtered Cu-K<sub>α</sub> radiation. WAXS profiles were collected in a scattering range of  $2\theta = 5$  to 70°, with a resolution of 0.02°, at a scanning speed of 2° min<sup>-1</sup>. Analyses were performed by applying an accelerating voltage of 40 kV and a current intensity of 30 mA.

### 2.4.4. Thermogravimetric analysis (TGA)

TGA analysis were carried out on a thermogravimetric analyzer (Netzsch, model STA 409PG/4/G Luxx, USA) at 10 °C min<sup>-1</sup> rate

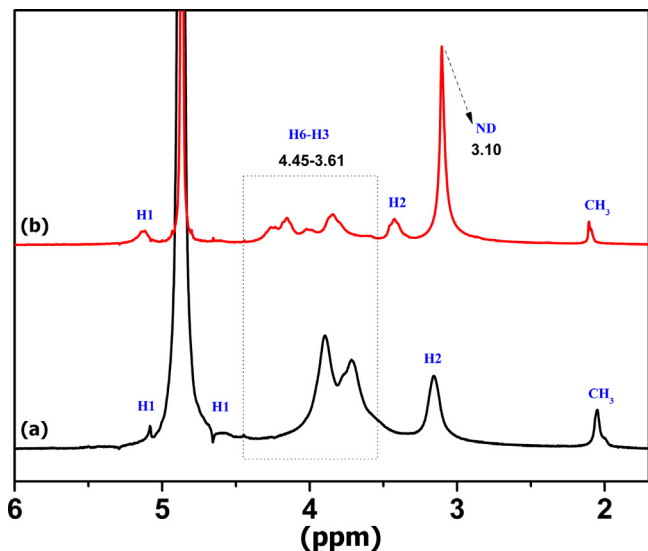


**Fig. 1.** <sup>1</sup>H NMR spectra of CHT (a) and DMC (b).

under nitrogen atmosphere with flow rate of 20 mL min<sup>-1</sup>, temperature ranged from 25 to 800 °C.

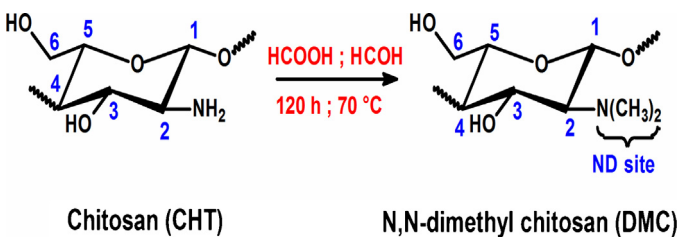
#### 2.4.5. In vitro heparin release

In vitro heparin (HP) release studies were performed in two different environments, both without the presence of enzymes: simulated intestinal fluid (SIF, 6.8 g of KH<sub>2</sub>PO<sub>4</sub> and 77 mL aqueous NaOH 0.20 mol L<sup>-1</sup> in 1000 mL of water, pH = 6.8); and simulated gastric fluid (SGF, 2.0 g NaCl and 7.0 mL of concentrated aqueous solution of HCl 37% (v/v) in 1000 mL of water, pH = 1.2) [2]. The releasing studies were carried out in a dissolutor apparatus Ethik Technology, model 299-6TS. For each run, 400 mg of dried PEC was deposited in a sealed flask with 400 mL of SIF or SGF. For each condition, the release study was carried out in duplicate (*n* = 2). So, each sample was kept under mild mechanical stirring (50 rpm), at 36.5 °C. At a desired time interval, an aliquot of 400 µL was removed from the flask and directly added to 5.0 mL of dimethyl-methylene blue (DMB) solution (pH ≈ 3.0) [2] for quantifying the amount of HP released by UV measurements (Shimadzu, UV mini 1240) at 525 nm. The absorbance related to DMB/heparin complex solution were performed immediately after homogenization of the system, according to methodology described by Martins et al. [2]. To quantify the solute released from PEC, one analytical curve (*R*<sup>2</sup> = 0.999) correlating the absorption of DMB/HP complex to HP concentration (1.0 to 50.0 mg L<sup>-1</sup>) using DMB solution as solvent, was built.

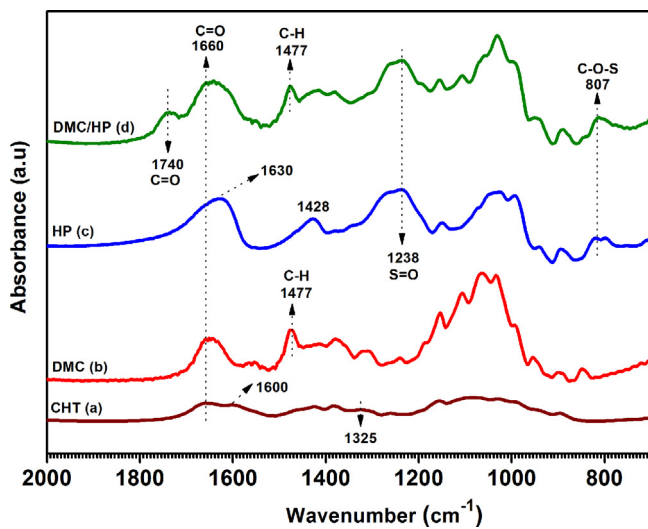
## 3. Results and discussion

### 3.1. Characterization of *N,N*-dimethyl chitosan by <sup>1</sup>H NMR

All the <sup>1</sup>H NMR signals were attributed and related to the structures of polysaccharides (Scheme 1). The differences in the <sup>1</sup>H NMR



**Scheme 1.** Synthetic route of DMC.

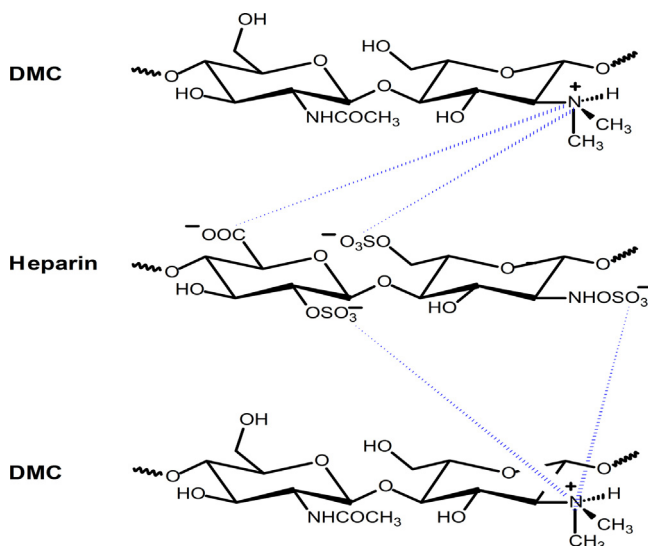


**Fig. 2.** FTIR spectra of CHT, DMC, HP and PEC.

spectra indicate the DMC was successfully obtained. The resonance signal at δ 2.05 ppm presented in the CHT <sup>1</sup>H NMR spectrum (Fig. 1a) was assigned to the hydrogen atoms of acetylated residues; the resonance at δ 3.16 ppm was assigned to the hydrogen atoms (H2); the resonances observed between δ 3.61 and δ 4.45 ppm were assigned to the hydrogen atoms (H3–H6) and resonances of low intensity that occur in the spectral range between δ 4.5 and δ 5.5 ppm were assigned to the hydrogen atoms (H1) [28–30]. However, the intense resonance in the spectral range δ 4.72 to δ 5.00 was attributed to hydrogen resonance of water molecules. DMC was obtained with dimethylation degree (DD) of ca. 86% [30,31]. The DD was obtained using Eq (1), from the area attributed to resonance of hydrogen atoms on *N*-dimethylated sites –N(CH<sub>3</sub>)<sub>2</sub>, at δ 3.10 ppm, and from area of H2 resonance at δ 3.43 ppm (Fig. 1b). The high value of DD for DMC (DD = 86%) confirmed the fully *N*-dimethylation of NH<sub>2</sub> groups of CHT since the acetylation degree of the CHT is ca. 15%.

### 3.2. Characterization of PECs by FTIR spectroscopy

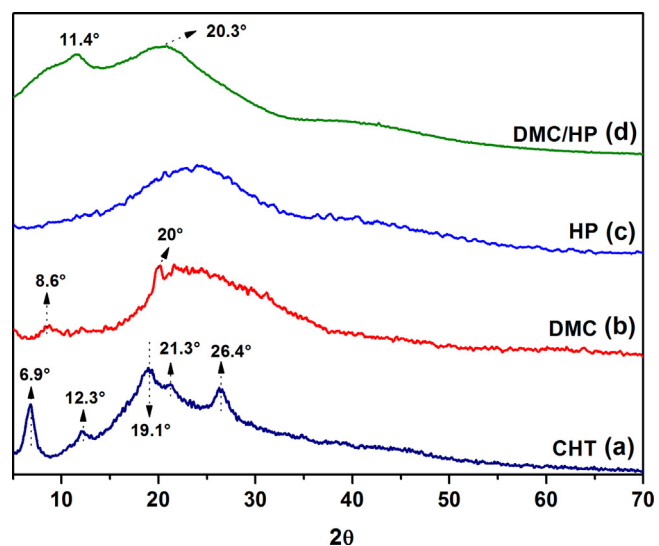
FTIR spectra of CHT, DMC, HP and PEC (DMC/HP) are shown in Fig. 2. The absorption that appears at 1600 cm<sup>-1</sup> refers to angular deformation of the N–H bonds (Fig. 2a). The absorption at 1661 and 1320 cm<sup>-1</sup> are characteristic of CHT and were assigned to amide I and III, respectively [32,33]. The band at 1477 cm<sup>-1</sup> was attributed to angular deformation of C–H bonds of methyl groups on DMC structure, which occurred due to methylation of CHT (Fig. 1b) [33]. The bands at 1630 cm<sup>-1</sup> and 1428 cm<sup>-1</sup> in the HP FTIR spectrum are assigned to the asymmetric and symmetric axial deformations of the carboxylate anion (–COO<sup>–</sup>) [2]. When compared to the FTIR spectrum of PEC, these bands have some changes due to complexation among HP and DMC chains. In the HP FTIR spectrum the bands at 1238 and 807 cm<sup>-1</sup> were assigned to asymmetric axial deformation of the S=O bonds and the axial deformation of C–O–S bonds, respectively [2]. The band at 1740 cm<sup>-1</sup> on PEC FTIR spectrum was attributed to the C=O bonds of carboxylic groups. HP is an anionic biopolymer that consists of α(1,4)-glycosidic linkages, to either D-glucuronic and L-iduronic acid. The pKa values of D-glucuronic, L-iduronic acid units are ca. 2.93 and 3.13, respectively [34]. Therefore, some of the carboxyl groups of HP on PEC structure remain non-ionized, since the PEC was obtained at pH 3.0. Therefore, the band at 1740 cm<sup>-1</sup> confirms the DMC/HP PEC formation. On the other hand, the band at 1740 cm<sup>-1</sup> on HP FTIR spectrum did not observe, whereas the raw HP was obtained as heparin sodium salt. In this case, carboxylate groups on heparin sodium salt structure are

**Scheme 2.** Physical structure of PEC based on DMC/HP at pH 3.0.

ionized. In addition, the PEC was obtained at pH 3.0 and this condition  $-\text{OSO}_3^-$  groups on HP backbone are ionized, whereas  $-\text{OSO}_3\text{H}$  pKa value is ca. 2.6 [35]. Therefore, the most likely structure of DMC/HP is depicted in **Scheme 2**.

### 3.3. WAXS analysis

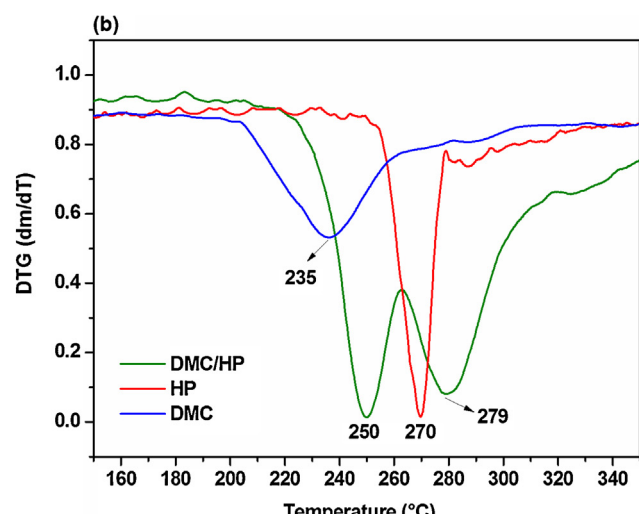
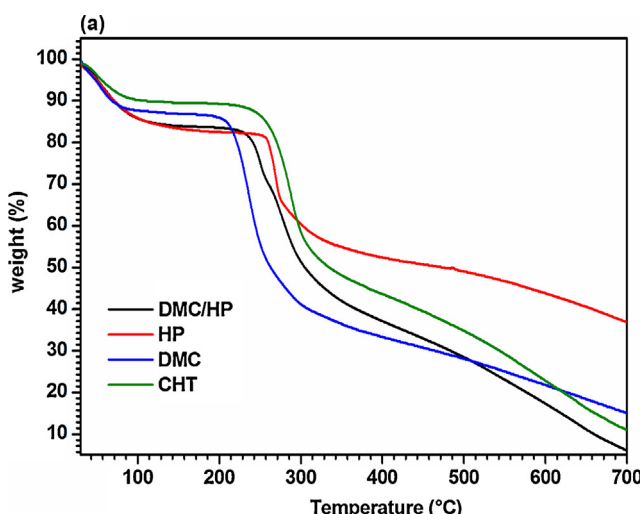
CHT WAXS profile (curve **a**) exhibited diffraction peaks at  $2\theta = 6.9^\circ$ ,  $12.3^\circ$ ,  $19.1^\circ$ ,  $21.3^\circ$ , and  $26.4^\circ$ . These crystalline domains occur due to high intensities of intermolecular H-bonds among hydroxyl and amino groups on CHT chain segments [36]. DMC WAXS profile (curve **b**) showed two broad peaks of low intensity at  $2\theta = 8.6^\circ$  and  $20^\circ$ . The insertion of methyl groups on CHT decreased the amount of intramolecular (DMC–DMC) H-bonds and, consequently, the DMC crystallinity was reduced as well as the crystalline structure that remained was changed, possibly due to PEC chains self-assembly. The absence of diffraction peaks at  $2\theta = 6.9^\circ$  and  $12.3^\circ$  (curve **b**) occurs due to full N-dimethylation of the amino groups on CHT [37]. HP WAXS profile (curve **c**) presented a broad peak of low intensity in the  $2\theta = 15^\circ$ – $30^\circ$  range. On the other hand, the PEC WAXS profile (curve **d**) showed two diffraction peaks

**Fig. 3.** WAXS profiles of CHT (a), DMC (b), HP (c) and PEC (d).

at  $2\theta = 11.4^\circ$  and  $20.3^\circ$ . The PEC was obtained from separately DMC and HP buffered solutions (at pH 3.0). This condition favors the association among DMC– $^+\text{NH}(\text{CH}_3)_2$  groups with the HP anionic sites, such as  $-\text{COO}^-$  and  $-\text{OSO}_3^-$  groups. These interactions promoted changes in the WAXS profiles, slightly increasing the PEC crystallinity, regarding unmodified HP and DMC.

### 3.4. TGA analysis

TGA curves of CHT, DMC, HP and PEC are shown in **Fig. 4a**. The first event of weight loss occurred in the 30–100 °C range, and it was attributed to evaporation of water and volatile compounds. All the samples presented similar amounts of adsorbed water (10 to 15 wt%). The second event of weight loss occurred between 200 and 350 °C and was attributed to the polysaccharides degradation (**Fig. 4a**). It was found that the CHT and HP are more thermally stable when compared to the PEC and DMC (**Fig. 4a**). The lower thermal stability of such samples comparing to CHT and HP occurs due to the high dimethylation content on CHT, i.e., due to insertion of methyl groups on CHT. The inclusion of these hydrophobic bulky groups (methyl groups) on CHT decreased the occurrence of

**Fig. 4.** TGA curves of CHT, DMC, HP and PEC (a) and DTG curves of DMC, HP and PEC (b).

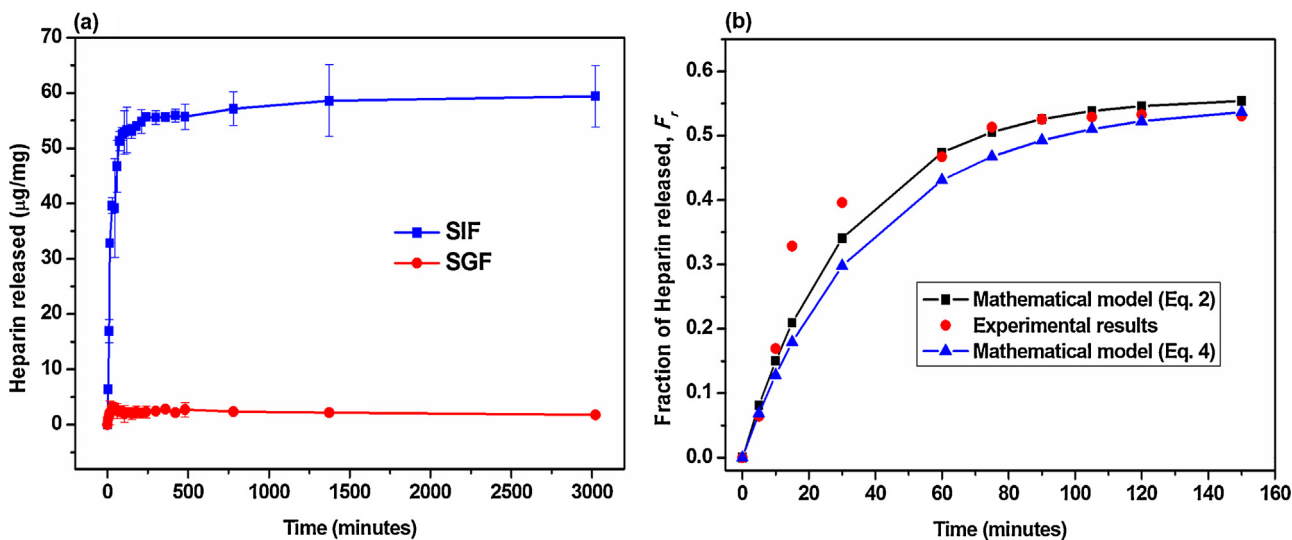


**Fig. 5.** Amount released of HP from PEC in SIF and SGF (Fig. 5a). Experimental and theoretical release profiles for HP obtained from mathematical models described by Eqs. (2) and (4) at 37 °C in SIF (Fig. 5b).

H-bonds among DMC–DMC chains, comparing to CHT–CHT segments [1,33]. The first derivatives of degradation stage (second event on TGA curves) for HP, DMC and PEC are presented in Fig. 4b. DMC/HP sample showed two degradation temperatures, as indicated by the inflection points at 250 and 279 °C (Fig. 4b) which are slightly higher than those observed for pure DMC (235 °C) and pure HP (270 °C). This fact confirms the PEC was obtained considering that the HP–DMC interactions provided higher thermal stability to the complex.

### 3.5. In vitro heparin release from PEC

HP releasing curves were obtained in SIF and SGF (Fig. 5a). The maximum fraction of HP released in SIF (at pH 6.8) was ca. 80 ± 1%, i.e., about 60 μg of HP per each milligram of PEC (60 μg mg<sup>-1</sup>). The equilibrium state was achieved after 250 min (Fig. 5a). In SGF medium (at pH 1.2), the fraction of HP released was lower than 5% (Fig. 5a), indicating that such PEC has potential to be used as a HP oral delivery device. PEC was obtained at pH 3.0 because at this condition the –N(CH<sub>3</sub>)<sub>2</sub> groups are protonated [–<sup>+</sup>NH(CH<sub>3</sub>)<sub>2</sub>] and can interact with HP anionic groups (–COO<sup>–</sup> and –OSO<sub>3</sub><sup>–</sup>) [34]. In SIF (pH 6.8) the –N(CH<sub>3</sub>)<sub>2</sub> groups did not protonate because the pKa of these sites is around 6.5 [2,6]. Therefore, HP can be easily released from PEC when the pH is equal or above 6.8. The –N(CH<sub>3</sub>)<sub>2</sub> sites are deprotonated in SIF and an amount of HP previously complexed with DMC molecules was released. On the other hand, in SGF (pH 1.2), the –N(CH<sub>3</sub>)<sub>2</sub> sites are ionized <sup>+</sup>NH(CH<sub>3</sub>)<sub>2</sub>, and the electrostatic interactions between DMC and HP prevail. This fact significantly reduces the amount of HP released.

The release and absorption rates of HP are correspondents when the condition of equilibrium is reached and the fractional release ( $F_r$ ) attains a maximum value ( $F_{max}$ ) for a given condition (Fig. 5a) [37,38]. The solute distribution between the hydrogel 3D matrix and the external fluid is defined by the  $\alpha$  parameter (partition activity), which can be used to evaluate the partition phenomena occurrence. In this case,  $\alpha$  parameter should reach a constant value at the equilibrium state and can be determined from the  $F_{max}$  value by the following equation [38]:

$$\alpha = \frac{F_{max}}{1 - F_{max}} \quad (2)$$

The physical and chemical affinity among solute, hydrogel matrix and external fluid is expressed by the  $\alpha$  parameter. The

solute diffusion from hydrogel into external fluid occurs when  $\alpha > 0$  [38]. So, the amount of HP released from hydrogel could be treated as a diffusion and/or partition phenomenon, because the  $\alpha$  value was 1.27, considering  $F_{max} = 0.559$  [37–39]. In this case,  $F_{max}$  and  $F_r$  parameters were obtained from release curve performed in SIF (pH 6.8), being the  $F_{max} = 0.559$  for the first 150 min of assay in SIF (Fig. 5a). Then, the kinetic constant of release ( $k_r$ ) could be determined, using the partition–diffusion mathematical model described by the following equations [38,39]:

$$F_{max} \ln \left( \frac{F_{max}}{F_{max} - F_r} \right) = k_r t \quad (3)$$

$$\frac{\alpha}{2} \ln \left( \frac{F_r - 2F_r F_{max} + F_{max}}{F_{max} + F_r} \right) = k_r t \quad (4)$$

In this case, the solute fraction released,  $F_r$ , in a given release time  $t$ , related to the first order reversible kinetic can be determined by Eq. (3), but if the release occurs through a second order reversible kinetic, Eq. (4) can be used to establish the  $F_r$  value [38]. So, the proposed models, described by Eqs. (3) and (4) were adjusted to the experimental data for the first 150 min of assay in SIF, where  $F_{max}$  reached 0.559 (Fig. 5b).

The curves obtained by the application of Eqs. (3) and (4) were superimposed to obtained experimental data, and the release kinetic in SIF was analyzed in the first 150 min of study (Fig. 5b). The value of  $k_r$  constant obtained was 0.075 min<sup>-1</sup> ( $R^2 = 0.99$ ) and the data described by Eq. (2) are in accordance with the experimental curve in SIF (Fig. 5a). Therefore, the experimental HP releasing profile is better explained by the first-order kinetic model, because when the second-order kinetic model was applied the  $k_r$  constant value obtained was 0.015 min<sup>-1</sup> ( $R^2 = 0.93$ ). Table 1 presents the values of  $k_r$  and  $R^2$  obtained from the curve shown in Fig. 5a, performed in SIF, after apply Eqs. (3) and (4).

**Table 1**

Values of  $k_r$  and  $R^2$  determined by the application of mathematical models described through Eqs. (3) and (4) from releasing curve of heparin (Fig. 5a) obtained in SIF (pH 6.8) at 37 °C.

Model	$k_r$ (min <sup>-1</sup> )	$R^2$
Eq. (3)	0.075	0.99
Eq. (4)	0.015	0.93

## 4. Conclusions

*N,N*-Dimethyl chitosan (DMC) was synthesized by methylation of chitosan (CHT) and the degree of dimethylation was determinate by <sup>1</sup>H NMR. Polyelectrolyte complex of DMC/heparin (DMC/HP) was obtained at pH 3.0. The materials were characterized by FTIR, WAXS and TGA/DTG analysis. Studies of controlled release of HP were performed on different environments (SGF and SIF). The results were satisfactory, since that 80% of HP-loaded was released on SIF (pH 6.8), after 250 min of assay. The release profile obtained in SIF followed a kinetic of first-order. This fact was confirmed by the partition-diffusion mathematical model described by Eq. (2). So, the PEC based on DMC/HP could release HP of high molecular weight (14,000 g mol<sup>-1</sup>) at pH close to physiological condition. By present such performance; the PEC has potential for act as an efficient vehicle for HP drug-carrier.

## Acknowledgments

The authors thank CNPq/CAPES, Brazil, for the financial support (Proc. 481424/2010-5 and Proc. 308337/2013-1).

## References

- [1] A.F. Martins, A.G.B. Pereira, A.R. Fajardo, A.F. Rubira, E.C. Muniz, Carbohydr. Polym. 86 (2011) 1266–1272.
- [2] A.F. Martins, J.F. Piai, I.T.A. Schuquel, A.F. Rubira, E.C. Muniz, Colloid Polym. Sci. 289 (2011) 1133–1144.
- [3] W.P. Novello, A.C. Arruda, M.H. Santana, A.M. Moraes, S.C. Pinho, J. Mater. Sci. Mater. Med. 9 (1998) 793–796.
- [4] J. Fu, J. Ji, W. Yuan, J. Shen, Biomaterials 26 (2005) 6684–6692.
- [5] J.M. Walenga, R.L. Bick, Med. Clin. N. Am. 82 (1998) 635–658.
- [6] A.F. Martins, D.M. de Oliveira, A.G.B. Pereira, A.F. Rubira, E.C. Muniz, Int. J. Biol. Macromol. 51 (2012) 1127–1133.
- [7] B.F. Choonara, Y.E. Choonara, P. Kumar, D. Bijukumar, L.C. du Toit, V. Pillay, Biotechnol. Adv. 32 (2014) 1269–1282.
- [8] F. Fabris, S. Ahmad, G. Celli, W.P. Jeske, J.M. Walenga, J. Fareed, Arch. Pathol. Lab. Med. 124 (2000) 1657–1666.
- [9] F. Fabris, G. Luzzatto, P.M. Stefani, B. Girolami, G. Celli, A. Girolami, Haematologica 85 (2000) 72–81.
- [10] J.R.S. Day, R.C. Landis, K.M. Taylor, J. Cardiothorac. Vas. Anesth. 18 (2004) 93–100.
- [11] L.B. Jaques, Science 206 (1979) 528–533.
- [12] J.K.W. Lam, Y. Xu, A. Worsley, I.C.K. Wong, Adv. Drug Delivery Rev. 73 (2014) 50–62.
- [13] S.C. Boca, M. Potara, A.-M. Gabudean, A. Juhem, P.L. Baldeck, S. Astilean, Cancer Lett. 311 (2011) 131–140.
- [14] A.F. Martins, S.P. Facchi, H.D.M. Follmann, A.G.B. Pereira, A.F. Rubira, E.C. Muniz, Int. J. Mol. Sci. 15 (2014) 20800–20832.
- [15] B. Lorkowska-Zawicka, K. Kaminski, J. Ciejska, K. Szczubialka, M. Bialas, K. Okon, D. Adamek, M. Nowakowska, J. Jawien, R. Olszanecki, R. Korbut, Mar. Drugs 12 (2014) 3953–3969.
- [16] A.M. Thomas, A.J. Gomez, J.L. Palma, W.T. Yap, L.D. Shea, Biomaterials 35 (2014) 8687–8693.
- [17] R. Subbiah, P. Ramalingam, S. Ramasundaram, D.Y. Kim, K. Park, M.K. Ramasamy, K.J. Choi, Carbohydr. Polym. 89 (2012) 1289–1297.
- [18] S.M. van der Merwe, J.C. Verhoeft, J.H.M. Verheijden, A.F. Kotze, H.E. Junginger, Eur. J. Pharm. Biopharm. 58 (2004) 225–235.
- [19] W. Sajomsang, P. Gonil, U.R. Ruktanonchai, M. Petchsangsai, P. Opanasopit, S. Puttipipatkhachorn, Carbohydr. Polym. 91 (2013) 508–517.
- [20] R.J.B. Pinto, S.C.M. Fernandes, C.S.R. Freire, P. Sadocco, J. Causio, C. Pascoal Neto, T. Trindade, Carbohydr. Res. 348 (2012) 77–83.
- [21] H.D. Follmann, A.F. Martins, A.P. Gerola, T.A. Burgo, C.V. Nakamura, A.F. Rubira, E.C. Muniz, Biomacromolecules 13 (2012) 3711–3722.
- [22] W. Huo, W. Zhang, W. Wang, X. Zhou, Int. J. Biol. Macromol. 70 (2014) 257–265.
- [23] J. Wu, S. Ding, J. Chen, S. Zhou, H. Ding, Int. J. Biol. Macromol. 68 (2014) 107–112.
- [24] Z. Wang, R. Zeng, M. Tu, J. Zhao, J. Appl. Polym. Sci. 128 (2013) 153–160.
- [25] A. Zhang, D. Ding, J. Ren, X. Zhu, Y. Yao, J. Appl. Polym. Sci. 131 (2014) 39890–39899.
- [26] S.M. van der Merwe, J.C. Verhoeft, A.F. Kotze, H.E. Junginger, Eur. J. Pharm. Biopharm. 57 (2004) 85–91.
- [27] A.F. Martins, P.V.A. Bueno, H.D.M. Follmann, S.R. Nocchi, C.V. Nakamura, A.F. Rubira, E.C. Muniz, Carbohydr. Res. 381 (2013) 153–160.
- [28] A.F. Martins, J.F. Piai, I.T.A. Schuquel, A.F. Rubira, E.C. Muniz, Colloid Polym. Sci. 289 (2011) 1133–1144.
- [29] D. de Britto, L.A. Forato, O.B.G. Assis, Carbohydr. Polym. 74 (2008) 86–91.
- [30] A.F. Martins, S.P. Facchi, J.P. Monteiro, S.R. Nocchi, C.T.P. Silva, C.V. Nakamura, E.M. Girotto, A.F. Rubira, E.C. Muniz, Int. J. Biol. Macromol. 72 (2015) 466–471.
- [31] A.F. Martins, S.P. Faccini, H.D.M. Follmann, A.P. Gerola, A.F. Rubira, E.C. Muniz, Carbohydr. Res. 402 (2015) 252–260.
- [32] T. Xu, M. Xin, M. Li, H. Huang, S. Zhou, J. Liu, Carbohydr. Polym. 346 (2011) 2445–2450.
- [33] T. Xu, M. Xin, M. Li, H. Huang, S. Zhou, Carbohydr. Polym. 81 (2010) 931–936.
- [34] H.M. Wang, D. Loganathan, R.J. Linhardt, Biochem. J. 278 (1991) 689–695.
- [35] J.F. Piai, A.F. Rubira, E.C. Muniz, Acta Biomater. 5 (2009) 2601–2609.
- [36] A.R. Fajardo, J.F. Piai, A.F. Rubira, E.C. Muniz, Carbohydr. Polym. 80 (2010) 934–943.
- [37] A.F. Martins, P.V.A. Bueno, E.A.M.S. Almeida, F.H.A. Rodrigues, A.F. Rubira, E.C. Muniz, Int. J. Biol. Macromol. 57 (2013) 174–184.
- [38] R.A. Bossoni, A.J.M. Valente, A.F. Rubira, E.C. Muniz, J. Braz. Chem. Soc. 25 (2014) 1124–1134.
- [39] A.V. Reis, M.R. Guilherme, A.F. Rubira, E.C. Muniz, J. Colloid Interface Sci. 310 (2007) 128–135.